Am J Cancer Res 2026;16(5):1745-1760
www.ajcr.us /ISSN:2156-6976/ajcr0173218

Original Article

GTPBP4 promotes colorectal cancer cell proliferation by positively regulating MYC-driven glycolytic metabolism

Kai Zhao, Jiayu Wei, Ying Shen, Anqi Jiang, Mingyang Gu, Jianzhong Deng

Department of Oncology, Wujin Hospital Affiliated to Jiangsu University, Changzhou 213017, Jiangsu, China

Received April 10, 2026; Accepted April 29, 2026; Epub May 15, 2026; Published May 30, 2026

Abstract: Colorectal cancer remains a leading cause of cancer death globally, creating an urgent need for novel therapeutic targets. Here, we investigate the expression, function, and regulatory mechanism of GTP-binding protein 4 (GTPBP4) in colorectal cancer. Analysis of The Cancer Genome Atlas (TCGA) colon adenocarcinoma (COAD) dataset showed that GTPBP4 is upregulated in colorectal tumors relative to normal mucosa, and high GTPBP4 expression correlates significantly with reduced overall survival. We observed a strong positive correlation between GTPBP4 and MYC expression across the cohort, leading us to generate stable GTPBP4-knockdown HCT116 and SW620 cells, as well as isogenic rescue lines overexpressing MYC. GTPBP4 depletion markedly suppressed cell proliferation, as determined by Cell Counting Kit-8 (CCK-8), 5-ethynyl-2'-deoxyuridine (EdU) incorporation, and clonogenic assays. Mechanistically, GTPBP4 knockdown reduced both MYC mRNA and protein levels, accelerated MYC protein turnover, and increased MYC ubiquitination (all $P < 0.05$), indicating dual transcriptional and post-translational regulation. Concurrently, GTPBP4 silencing downregulated key glycolytic enzymes and decreased glycolytic flux, effects that were fully reversed by ectopic MYC expression ($P < 0.05$). In a subcutaneous xenograft model, GTPBP4 knockdown significantly inhibited tumor growth, reduced MYC and Ki-67 proliferation antigen (Ki-67) expression, and blunted glycolytic metabolism ($P < 0.01$ or $P < 0.05$). Co-expression of MYC restored all these parameters and reversed the enhanced MYC ubiquitination ($P < 0.05$). Collectively, our data demonstrate that GTPBP4 sustains MYC expression through dual mechanisms to drive glycolytic reprogramming and colorectal cancer growth, identifying the GTPBP4/MYC/glycolysis axis as a promising therapeutic target.

Keywords: Colorectal cancer, MYC, ubiquitination, glycolysis

Introduction

According to data from the International Agency for Research on Cancer (IARC), colorectal cancer (CRC) ranks as the second leading cause of cancer-related mortality among both men and women globally. In 2022, nearly one million deaths were attributed to this malignancy worldwide [1]. Therapeutic options for CRC currently remain limited: cytotoxic chemotherapy is largely confined to oxaliplatin, irinotecan, and fluoropyrimidines; anti-angiogenic agents include bevacizumab, regorafenib, and fruquintinib; and targeted therapy directed against the epidermal growth factor receptor (EGFR) is restricted to cetuximab. For patients with advanced CRC who remain candidates for continued antineoplastic therapy, the paucity of available regimens directly compromises survival outcomes [2]. Consequently, the identification of novel therapeutic targets to improve survival rates among CRC patients has become increasingly imperative. Rapid advances in high-throughput sequencing and gene microarray technologies have accelerated the analysis of genetic data, leading to the continual discovery of genes implicated in the initiation and progression of CRC [3].

Members of the guanosine triphosphate binding protein (GTPBP) family function as guanosine triphosphatases (GTPases), hydrolyzing GTP from an active GTP-bound state to an inactive guanosine diphosphate (GDP)-bound state [4]. GTP binding protein 4 (GTPBP4) is a relatively recent addition to the GTPase family and participates in the biogenesis and maturation of the 60S ribosomal subunit, processes intimate-

https://doi.org/10.62347/OKYW9037

ly linked to cell proliferation and growth [5]. Previous studies have documented that upregulation of GTPBP4 promotes proliferation in hepatocellular carcinoma cells [6], gastric cancer cells [7], and breast cancer cells [8]. In lung cancer, silencing GTPBP4 markedly suppresses cell proliferation, angiogenesis, colony formation, and tumor progression in nude mice [9].

Glycolysis constitutes a central factor in cancer progression [10]. Whereas normal cells primarily rely on mitochondrial oxidative phosphorylation for energy production under aerobic conditions, tumor cells exhibit a heightened dependence on glycolysis even in the presence of oxygen, a phenomenon known as the Warburg effect [11]. During glycolysis, lactate dehydrogenase A (LDHA) catalyzes the conversion of pyruvate to lactate. Lactate accumulation acidifies the extracellular microenvironment, thereby fostering malignant proliferation and tumor growth [12]. The MYC proto-oncogene protein (MYC) plays a pivotal role in orchestrating aerobic glycolysis by directly activating the transcription of nearly all glycolytic genes through binding to canonical E-box sequences, including glucose transporter 1 (*GLUT1*), hexokinase 2 (*HK2*), and *LDHA* [13].

Ubiquitin (Ub), a 76-amino acid polypeptide present in all eukaryotic tissues, together with its degradation pathway via the proteasome, constitutes the ubiquitin-proteasome system (UPS) [14]. This tightly regulated system governs intracellular protein degradation and modulates diverse cellular processes, including cell cycle progression, deoxyribonucleic acid (DNA) damage repair, signal transduction, immune responses, and oxidative stress reactions [15]. Ubiquitination, a prevalent post-translational modification in eukaryotes, involves the covalent attachment of ubiquitin to target substrates [16]. In cancer, ubiquitination can exert context-dependent regulation over both tumor-suppressive and oncogenic pathways [17].

Through bioinformatic analysis of clinical and transcriptomic data from The Cancer Genome Atlas (TCGA) database, we observed that GTPBP4 is highly expressed in colon adenocarcinoma (COAD). Correlation analysis between GTPBP4 and MYC revealed a significant positive association. Accordingly, this study further investigated the regulatory relationship between GTPBP4 and MYC. Our findings demonstrate that GTPBP4 preserves MYC protein stability by inhibiting its ubiquitin-mediated proteasomal degradation while concurrently exerting positive regulation on MYC transcription. Knockdown of GTPBP4 not only reduces MYC expression in colon adenocarcinoma cells but also diminishes glycolytic metabolite production, ultimately restraining both in vitro and in vivo growth of colon adenocarcinoma.

Materials and methods

Data collection

Transcriptome profiling data in TXT format and corresponding clinical annotations in XML format for colon adenocarcinoma (COAD) were retrieved from The Cancer Genome Atlas (TCGA) database (https://portal.gdc.cancer.gov/). Raw transcriptomic files were processed into a gene expression matrix using R software (version 4.4.3) and subsequently converted to Excel format for downstream analyses.

Gene screening

Bioinformatic analyses were executed using R software (version 4.4.3). Expression values for GTP binding protein 4 (GTPBP4) were extracted to characterize its pan-cancer expression landscape across diverse human malignancies relative to corresponding normal tissues. Differential expression of GTPBP4 between colon adenocarcinoma specimens and adjacent non-tumor mucosa was assessed. Kaplan-Meier survival analysis was performed with the 'Survival' package, and statistical significance was evaluated using the log-rank test to determine the association between GTPBP4 transcript abundance and overall patient survival.

Cell culture and cell transfection

Human colorectal cancer cell lines HCT116 and SW620 were obtained from the American Type Culture Collection (ATCC). Both lines were maintained in Dulbecco's Modified Eagle Medium (DMEM; Gibco) supplemented with 10% fetal bovine serum (FBS; Gibco) and 1% penicillin/streptomycin. Cultures were incubated at 37°C in a humidified atmosphere containing 5% carbon dioxide (CO_2). All experiments were performed using cells in the loga-

rithmic growth phase. Short hairpin RNA (shRNA) constructs targeting GTPBP4 (GTPBP4-shRNA), a non-targeting negative control shRNA (NC-shRNA), and the pcDNA3.1-MYC overexpression plasmid were synthesized by Sangon Biotech (Shanghai). A recombinant lentiviral vector expressing green fluorescent protein (GFP), pGSIL-shGTPBP4, was employed; the targeting sequence was 5'-GCTGGAGAGTATGACAGTGTActcgagTACACTGTCATACTCTCCAGC-3'. Lentiviral particles were generated by co-transfection of the shGTPBP4 plasmid with packaging plasmids psPAX2 and pMD2G. Stable cell lines were established via fluorescence-activated cell sorting (FACS) for GFP-positive cells following transduction. For MYC rescue experiments, the pcDNA3.1-c-Myc overexpression plasmid (Addgene) was utilized. Transfections were performed using Lipofectamine 3000 reagent (Invitrogen). Briefly, HCT116 cells in logarithmic growth were seeded into 6-well plates and allowed to reach 60-70% confluence. Cells were transfected with either NC-shRNA or GTPBP4-shRNA vectors to generate control and knockdown stable lines, respectively. Subsequently, the GTPBP4-shRNA stable line was transfected with the pcDNA3.1-MYC plasmid to establish the rescue group.

Animal model construction and grouping

Male BALB/c athymic nude mice, aged 4-6 weeks and weighing 18-22 g, were procured from Beijing Vital River Laboratory Animal Technology Co., Ltd. All animal experiments were approved by the Institutional Animal Care and Use Committee of Jiangsu University (Approval No. UJS-IACUC-AP-2025030443) and performed in strict accordance with the guidelines for the care and use of laboratory animals. Animals were maintained under specific pathogen-free (SPF) conditions with a 12-hour light/dark cycle, ambient temperature of 22 ± 2°C, and relative humidity of 50 ± 5%. Following a one-week acclimatization period, mice were randomly allocated into three groups (n = 8 per group) using a random number table: negative control short hairpin RNA (NC-shRNA) group, GTP binding protein 4 short hairpin RNA (GTPBP4-shRNA) knockdown group, and GTPBP4-shRNA plus MYC proto-oncogene protein (MYC) overexpression rescue group. Stably transfected cells in logarithmic growth phase were harvested and resuspended in serum-free Dulbecco's Modified Eagle Medium (DMEM) at a density of 5×10^6 cells per 100 μL. The cell suspension was injected subcutaneously into the right dorsal flank of each mouse. Euthanasia was performed via intraperitoneal administration of sodium pentobarbital (150 mg/kg) (P3761, Sigma-Aldrich). Tumor xenografts were excised intact and weighed. Portions of the tumor tissue were snap-frozen for subsequent ribonucleic acid (RNA) and protein extraction, while the remaining tissue was fixed in 4% paraformaldehyde, embedded in paraffin, and sectioned for immunohistochemical analysis.

Immunohistochemical staining

Paraffin-embedded tissue specimens were obtained from the archives of the Department of Pathology, encompassing 10 cases of colorectal cancer and matched adjacent normal mucosa (sampled ≥ 5 cm from the tumor margin) collected between January 2022 and December 2023. None of the patients had received preoperative radiotherapy, chemotherapy, targeted therapy, or any other antineoplastic intervention, and complete clinicopathological data were available for all cases. This study was approved by the Ethics Committee of Changzhou Wujin People's Hospital (Approval No. 2024-SR-128). The requirement for written informed consent was formally waived by the committee, given the exclusive use of fully anonymized archival pathological specimens that preclude patient identification and the absence of any potential harm, privacy violation, or impact on patient rights.

Immunohistochemical (IHC) staining was performed on sections of normal colon tissue, colorectal cancer tissue, and xenograft tumor tissue. Sections were deparaffinized in xylene and rehydrated through a graded ethanol series. Antigen retrieval was achieved by heating the slides in Tris-ethylenediaminetetraacetic acid (EDTA) buffer for 15 minutes, followed by incubation in 0.3% hydrogen peroxide-methanol solution for 10 minutes to quench endogenous peroxidase activity. After blocking with 5% bovine serum albumin (BSA) for 30 minutes at room temperature, sections were incubated overnight at 4°C with primary antibodies: anti-GTPBP4 (Fine Test, 1:100), anti-MYC (Cell Signaling Technology, 1:100), anti-Ki-67 (Abcam, 1:100), and anti-lactate dehydrogenase

A (LDHA) (ProteinTech, 1:100). Sections were subsequently incubated with horseradish peroxidase (HRP)-conjugated secondary antibody (Sangon Biotech, 1:100) for 60 minutes at room temperature. Immunoreactivity was visualized using a 3,3'-diaminobenzidine (DAB) chromogenic kit (Sangon Biotech), and nuclei were counterstained with hematoxylin. Images were captured using an inverted microscope at 20× magnification. All stained sections were evaluated independently by two experienced pathologists under blinded conditions. In instances of scoring discrepancy, a consensus was reached through joint re-examination and discussion.

Western blotting

Total ribonucleic acid (RNA) was extracted from cultured cells and xenograft tumor tissues using a Rapid RNA Extraction Kit (Yeasen Biotechnology). Complementary deoxyribonucleic acid (cDNA) was synthesized via reverse transcription. Quantitative polymerase chain reaction (qPCR) amplification was carried out in a 20 μL reaction volume comprising: 10 μL of 2× Hieff UNICON® Universal Blue qPCR SYBR Green Master Mix (Yeasen, Cat. No. 11184ES08), 0.4 μL each of forward and reverse primers (10 μmol/L), 2 μL of cDNA template, and 7.2 μL of nuclease-free water. Human glyceraldehyde-3-phosphate dehydrogenase (*GAPDH*) served as the internal reference control for assessing GTPBP4 and MYC expression. Thermal cycling conditions consisted of an initial denaturation at 95°C for 5 minutes, followed by 30 cycles of 94°C for 30 seconds, 52°C for 30 seconds, and 72°C for 30 seconds, with a final extension at 72°C for 5 minutes. Each sample was assayed in triplicate technical replicates. Relative gene expression levels were calculated using the 2^(-ΔΔCt) method. Primer sequences were as follows: *GTPBP4* forward, 5'-AGTTGCTCTCGAACTCCACG-3' and reverse, 5'-TGTCTATCCGCCTCCCCTTT-3'; MYC forward, 5'-AGCAGCGACTCTGAGGAGGAAC-3' and reverse, 5'-TCCAGCAGAAGGTGATCCAGACTC-3'; *GAPDH* forward, 5'-GTCTCCTCTGACTTCAACAGCG-3' and reverse, 5'-ACCACCCTGTTGCTGCTGTAGCCAA-3'.

Quantitative real-time PCR (qRT-PCR)

Total RNA was extracted from cells and xenograft tissues using an RNA extraction kit (Yisheng Biotechnology), and reverse transcribed into complementary DNA (cDNA). The expression levels of GTPBP4 and MYC were detected using human GAPDH as the internal reference. PCR amplification conditions were: pre-denaturation at 95°C for 5 min; 30 cycles of denaturation at 94°C for 30 s, annealing at 52°C for 30 s, and extension at 72°C for 30 s; final extension at 72°C for 5 min.

CCK-8 assay

Cell proliferation was assessed using the Cell Counting Kit-8 (CCK-8) reagent (Beyotime, China) for HCT116, HCT116-shGTPBP4, SW-620, and SW620-shGTPBP4 cells seeded in 96-well plates. At 24 h, 48 h, and 72 h time points, 10% CCK-8 reagent was added to each well, and the absorbance was measured at 450 nm using a microplate reader.

EdU assay

HCT116 and SW620 cells in the logarithmic growth phase were resuspended to a density of 2×10^5 cells/ml and seeded into 96-well plates. After overnight incubation to allow cell attachment, EdU was diluted to 20 μM, and 100 μl of the working solution was added to each well (final concentration 10 μM), followed by incubation at 37°C for 2 hours. Cells were fixed with 4% paraformaldehyde for 30 minutes and washed 1-2 times with PBS. The reaction solution was added, and cells were incubated at room temperature in the dark for 30 minutes to allow fluorescent dye binding to EdU. Images were captured using a fluorescence microscope or confocal microscope. The number of EdU-positive cells or fluorescence intensity was quantified to assess cell proliferation.

Colony formation assay

To assess the long-term proliferative capacity of colorectal cancer cells, HCT116 and SW620 cells were seeded into 6-well plates at densities of 4×10^3 and 1×10^3 cells per well, respectively. Cells were maintained in complete DMEM medium in a humidified incubator at 37°C with 5% CO_2, and the medium was refreshed every 3 days. After 14 days of culture, colonies were fixed with 4% paraformaldehyde for 15 min at room temperature, stained with 0.1% crystal violet solution for 20 min, and rinsed thoroughly with tap water to remove

excess stain. Plates were air-dried, and colonies containing more than 50 cells were counted manually under an inverted microscope.

In vivo and in vitro ubiquitination assay

Ubiquitination levels of MYC were determined by immunoprecipitation (IP) assay. Briefly, 293T cells or frozen subcutaneous xenograft tissues were lysed on ice for 30-45 min in radioimmunoprecipitation assay (RIPA) buffer supplemented with 1× protease inhibitor cocktail and 1× deubiquitinase inhibitor cocktail (Beyotime Biotechnology, Shanghai, China). Lysates were centrifuged at 14,000×g for 20 min at 4°C to remove cell debris, and the supernatants were collected. Protein concentrations were quantified using the BCA protein assay kit. For pre-clearing, 500 μg of total protein was incubated with 20 μL of Protein A/G agarose beads (Millipore, Billerica, MA, USA) at 4°C for 1 h to eliminate non-specific binding. The beads were removed by centrifugation, and the supernatants were incubated with 2 μg of anti-MYC antibody (Cell Signaling Technology, Cat# 9402, 1:1000) overnight at 4°C with gentle rotation. Subsequently, 50 μL of fresh Protein A/G agarose beads were added and incubated for an additional 4 h at 4°C. The beads were washed 5 times with cold RIPA buffer, and bound proteins were eluted by boiling in 2× SDS loading buffer for 10 min. Ubiquitinated MYC was detected by Western blotting using an anti-ubiquitin antibody (Cell Signaling Technology, Cat# 3936, 1:1000). Equal amounts of whole-cell lysates were loaded as input controls to confirm equal protein loading and to detect total MYC and total ubiquitin levels.

Detection of glycolytic metabolites

Pyruvate and lactate assay kits were purchased from SolarBio Life Sciences (BC2205, BC2235). The o-toluidine glucose assay kit was purchased from Beyotime Biotech (S0201S). All assays were performed strictly according to the manufacturers' instructions. Absorbance was read using an ELx800 multimode microplate reader (Bio Tek, USA) with appropriate reference wavelengths.

Statistical analysis

All experimental data are presented as mean ± standard deviation (SD). Statistical analyses were conducted using GraphPad Prism 8 software. Repeated measures analysis of variance (ANOVA) was employed to compare differences among groups. Pairwise comparisons between two groups were performed using independent-samples Student's *t*-tests. For comparisons involving three or more groups, one-way ANOVA was applied, followed by Tukey's post hoc test for multiple comparisons. All experiments were independently repeated a minimum of three times. A *P*-value of less than 0.05 was considered statistically significant.

Results

GTPBP4 is highly expressed in COAD

To delineate the expression profile of GTPBP4 in colorectal cancer, we first interrogated its pan-cancer landscape using the TCGA-COAD dataset. As illustrated in **Figure 1A**, GTPBP4 exhibited elevated transcript levels in tumor tissues relative to normal counterparts across a broad spectrum of malignancies, including bladder urothelial carcinoma (BLCA), breast invasive carcinoma (BRCA), cervical squamous cell carcinoma (CESC), cholangiocarcinoma (CHOL), colon adenocarcinoma (COAD), esophageal carcinoma (ESCA), glioblastoma multiforme (GBM), head and neck squamous cell carcinoma (HNSC), liver hepatocellular carcinoma (LIHC), lung adenocarcinoma (LUAD), lung squamous cell carcinoma (LUSC), prostate adenocarcinoma (PRAD), rectum adenocarcinoma (READ), stomach adenocarcinoma (STAD), thyroid carcinoma (THCA), and uterine corpus endometrial carcinoma (UCEC). Within the colorectal cancer cohort specifically, GTPBP4 expression was markedly elevated in tumor tissues compared with adjacent normal mucosa (**Figure 1B**). Kaplan-Meier survival analysis revealed that patients harboring high GTPBP4 expression had a significantly shorter overall survival duration than those with low expression (**Figure 1C**). Concordantly, immunohistochemical (IHC) staining confirmed robust GTPBP4 protein expression in colorectal cancer specimens (**Figure 1D**), and immunoblotting further validated substantially higher GTPBP4 protein levels in tumor lysates relative to paired normal tissues (**Figure 1E**). Assessment of endogenous GTPBP4 levels across a panel of colorectal cancer cell lines demonstrated pronounced expression in HCT116 and

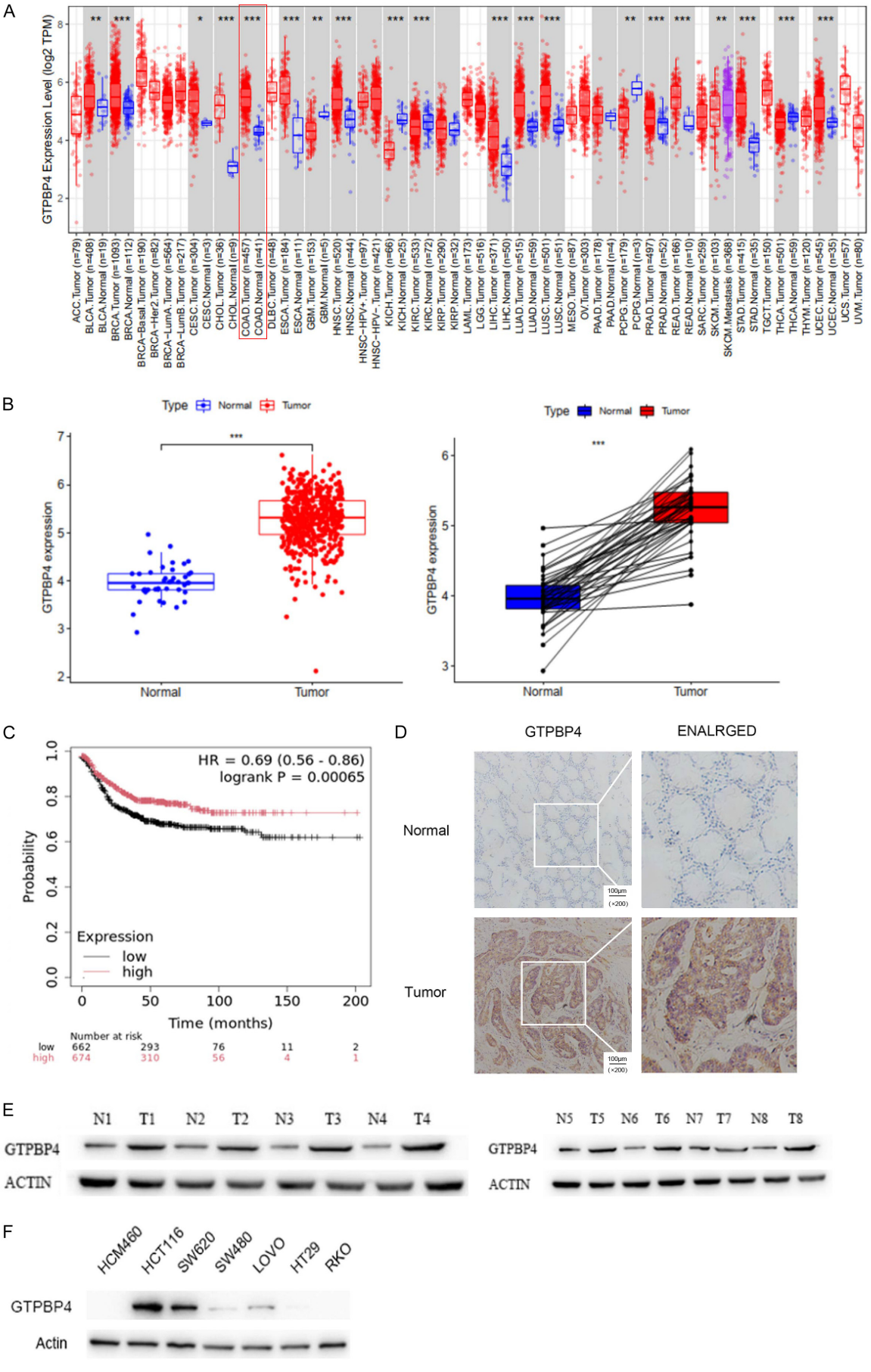
A
GTPBP4 Expression Level (log2 TPM)
B
Type Normal Tumor
GTPBP4 expression
Normal
Tumor
C
HR = 0.69 (0.56 - 0.86)
logrank P = 0.00065
Probability
Expression
low
high
Time (months)
Number at risk
low 662 293 76 11 2
high 674 310 56 4 1
D
GTPBP4
ENALRGED
Normal
Tumor
E
N1 T1 N2 T2 N3 T3 N4 T4
N5 T5 N6 T6 N7 T7 N8 T8
GTPBP4
ACTIN
F
HCM460 HCT116 SW620 SW480 LOVO HT29 RKO
GTPBP4
Actin

Figure 1. GTP-binding protein 4 (GTPBP4) was highly expressed in COAD. A: Pan-cancer analysis of GTP binding protein 4 (GTPBP4) expression across The Cancer Genome Atlas (TCGA) dataset. B: Comparative expression of GTPBP4 in colon adenocarcinoma (COAD) tissues versus adjacent non-tumor mucosa. C: Kaplan-Meier overall survival curves for COAD patients stratified by median GTPBP4 transcript abundance in the TCGA-COAD cohort. D: Representative immunohistochemistry (IHC) staining for GTPBP4 in normal colonic epithelium and colon adenocarcinoma tissue (scale bar = 100 μm, original magnification ×200). E: Immunoblot analysis of GTPBP4 protein levels in matched colon adenocarcinoma (T) and adjacent non-tumor (N) tissue pairs. F: Immunoblot assessment of endogenous GTPBP4 protein across a panel of colonic epithelial and colorectal cancer cell lines (NCM460, HCT116, SW620, SW480, LOVO, HT-29, RKO). $^{*}P < 0.05$, $^{**}P < 0.01$, $^{***}P < 0.001$.

SW620 cells (**Figure 1F**), which were therefore selected for subsequent functional and mechanistic interrogation.

Knockdown of GTPBP4 suppresses colorectal cancer cell proliferation

To further validate the functional role of GTP binding protein 4 (GTPBP4) in colorectal cancer, we established stable GTPBP4-knockdown derivatives of HCT116 and SW620 cells. Successful depletion of GTPBP4 was confirmed at the protein level by immunoblotting (**Figure 2A**) and at the transcript level by quantitative real-time polymerase chain reaction (qRT-PCR) (**Figure 2B**). Assessment of cell viability using the Cell Counting Kit-8 (CCK-8) assay at 24, 48, and 72 hours post-seeding revealed that GTPBP4-depleted cells exhibited markedly reduced viability relative to negative control short hairpin RNA (NC-shRNA)-transduced counterparts (**Figure 2C**). 5-ethynyl-2'-deoxyuridine (EdU) incorporation assays more directly demonstrated that GTPBP4 silencing curtailed the proliferative capacity of colorectal cancer cells (**Figure 2D**). In clonogenic assays, GTPBP4-knockdown cells generated fewer and smaller colonies compared with control cells (**Figure 2E**). Collectively, these findings indicate that depletion of GTPBP4 attenuates colorectal cancer cell proliferation.

GTPBP4 positively regulates MYC expression and modulates its protein stability

Correlation analysis between GTPBP4 and the MYC proto-oncogene protein (MYC) revealed a significant positive association (**Figure 3A**). We therefore sought to elucidate the regulatory relationship between GTPBP4 and MYC expression, as well as the underlying mechanism. Immunoblotting demonstrated that MYC protein abundance was substantially lower in GTPBP4-shRNA cells than in NC-shRNA controls (**Figure 3B**), and a concordant reduction was observed at the transcript level (**Figure 3C**). Ectopic expression of MYC in the GTPBP4-shRNA background via transfection of a *MYC*-encoding plasmid resulted in markedly elevated MYC protein levels compared with those in GTPBP4-shRNA cells alone (**Figure 3D**). To assess the rate of MYC degradation, control and HCT116-shGTPBP4 cells were treated with the protein synthesis inhibitor cycloheximide (CHX) for varying durations and subsequently analyzed by immunoblotting. The results indicated that GTPBP4 depletion shortened the half-life of MYC protein (**Figure 3E**). Treatment of GTPBP4-knockdown cells with either the autophagy inhibitor chloroquine (CQ) or the proteasome inhibitor MG132, followed by immunoblot analysis, suggested that the ubiquitin-proteasome pathway constitutes the principal route of MYC degradation (**Figure 3F**). Furthermore, exposure to MG132 for 0, 1, 2, and 4 hours led to a time-dependent accumulation of MYC protein (**Figure 3G**). Notably, combined GTPBP4 knockdown and MYC overexpression reduced the level of ubiquitinated MYC (**Figure 3H**).

Taken together, these data establish that GTPBP4 expression positively correlates with MYC levels. Depletion of GTPBP4 diminishes both MYC transcript and protein abundance in colorectal cancer cells, concurrently enhancing MYC ubiquitination and accelerating its proteasomal turnover. These observations support a model in which endogenous GTPBP4 restrains MYC ubiquitination and thereby contributes to the maintenance of MYC protein stability.

GTPBP4 activates glycolysis through MYC

To ascertain whether GTPBP4 participates in MYC-mediated reprogramming of glycolytic metabolism, we first examined the expression of glycolytic enzymes in GTPBP4-depleted cells. Immunoblot analysis revealed a pronounced reduction in the protein levels of lactate dehy-

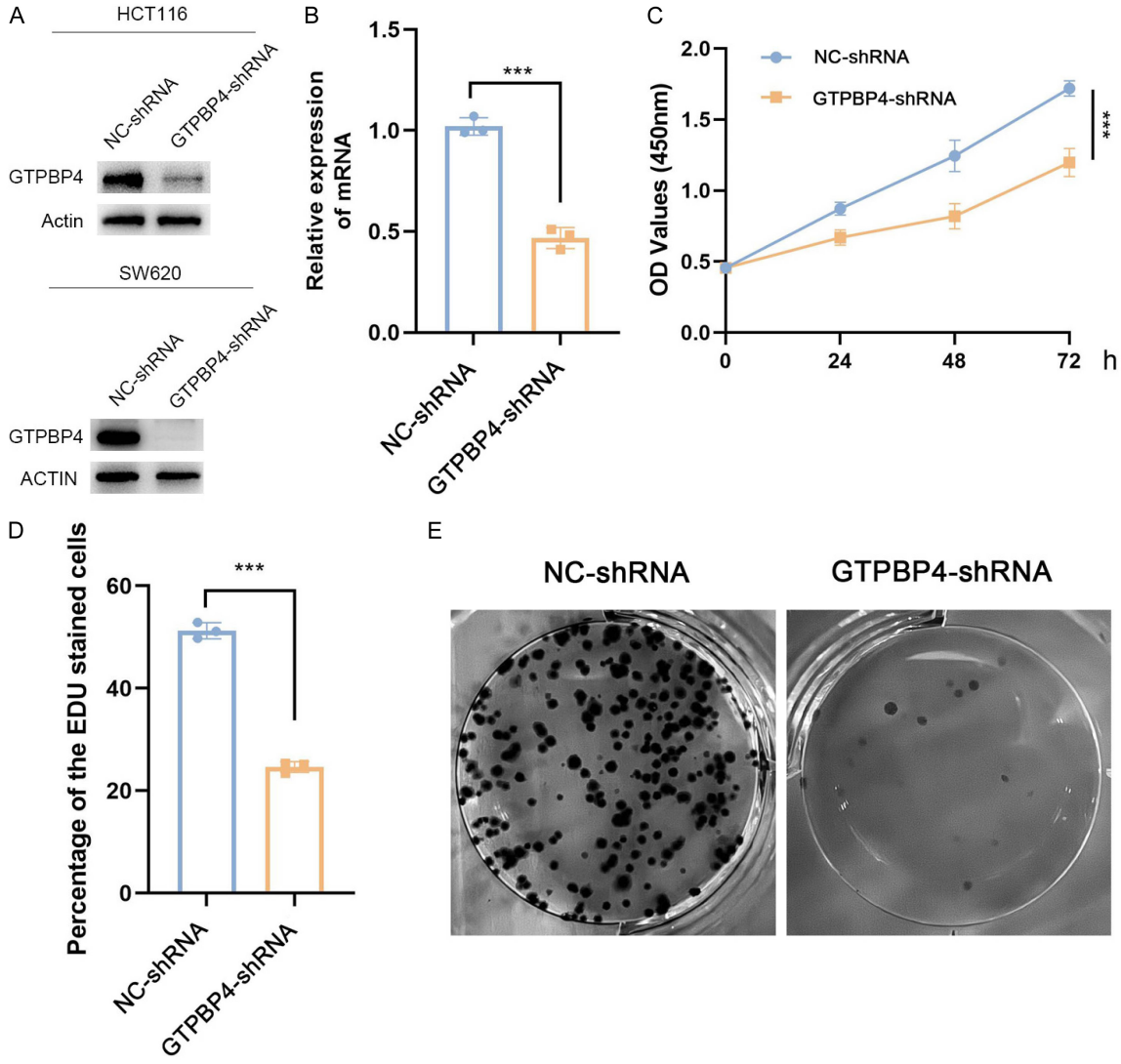

Figure 2. GTPBP4 knockdown inhibited colon cancer cell proliferation. A: Western blot analysis of GTPBP4 protein expression in colon cancer cell lines (HCT116-shGTPBP4 and SW620-shGTPBP4) with stable GTPBP4 knockdown. B: Quantitative real-time polymerase chain reaction (qRT-PCR) measurement of relative GTPBP4 messenger RNA (mRNA) abundance following lentiviral-mediated stable knockdown. C: Cell Counting Kit-8 (CCK-8) assay monitoring the proliferation kinetics of control and GTPBP4-depleted cells in vitro. D: 5-ethynyl-2'-deoxyuridine (EdU) incorporation assay quantifying DNA synthesis in control versus GTPBP4-knockdown cells. E: Representative images and quantification of colony formation assays illustrating the clonogenic capacity of control and GTPBP4-deficient cells. ***$P < 0.001$.

drogenase A (LDHA), phosphofructokinase platelet type (PFKP), and hexokinase 1 (HK1) in shGTPBP4 cells relative to controls (**Figure 4A**). Measurement of glycolytic end-products and intermediates showed that lactate production, pyruvate generation, and glucose consumption were all diminished in the GTPBP4-knockdown setting (**Figure 4B**). Importantly, reintroduction of MYC into GTPBP4-depleted cells (shGTPBP4+MYC) partially restored intracellular lactate and pyruvate levels, as well as glucose consumption, when compared with cells harboring GTPBP4 knockdown alone (**Figure 4C**).

In vivo validation of GTPBP4 and MYC involvement in colorectal cancer growth and glycolytic metabolism

To substantiate the functional relevance of the GTPBP4/MYC axis in colorectal cancer progression in vivo, we employed a subcutaneous

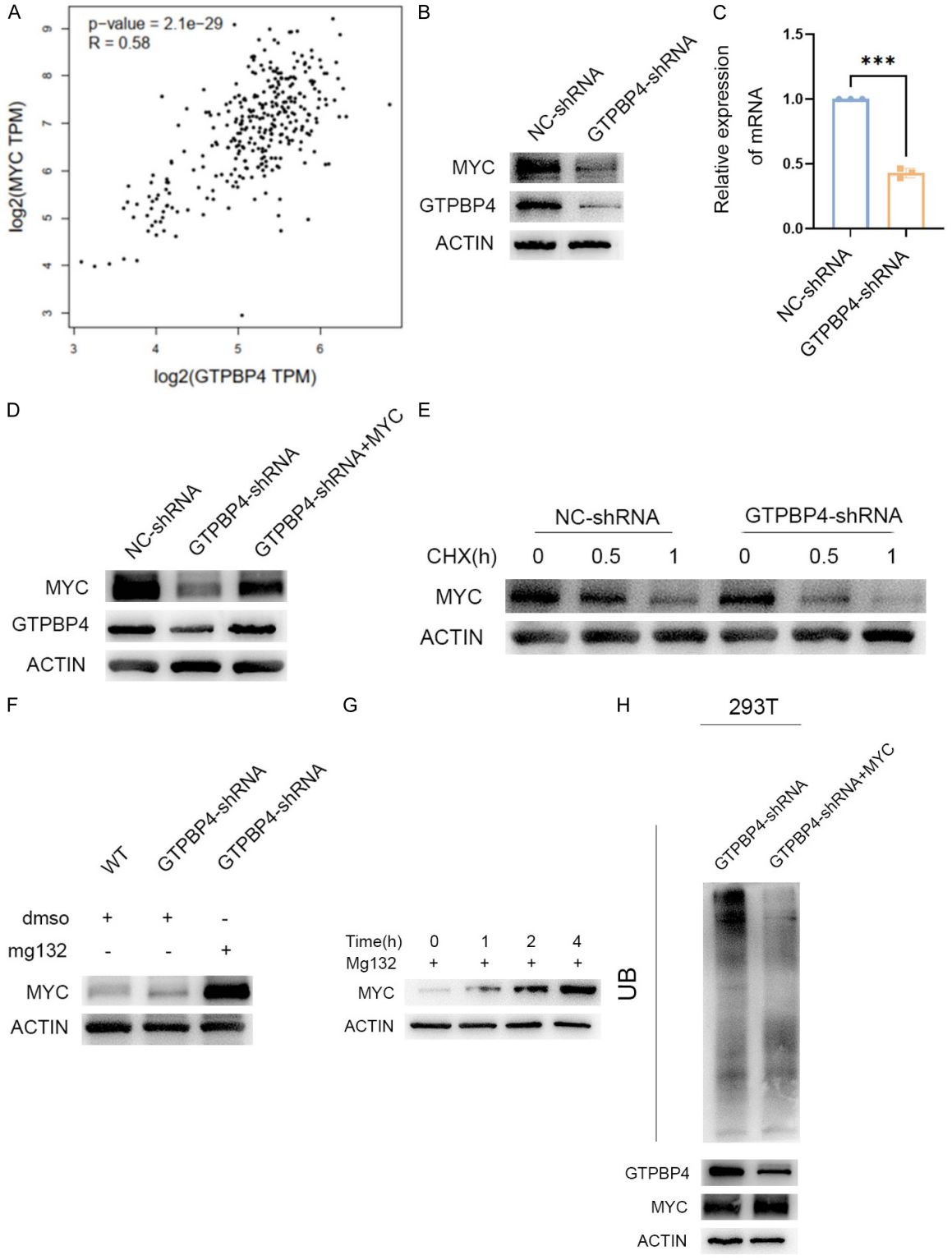

Figure 3. GTPBP4 regulates MYC protein degradation via the ubiquitin-proteasome pathway. A: Correlation scatter plot depicting the relationship between GTPBP4 and MYC proto-oncogene protein (MYC) transcript expression. B: Immunoblot analysis of MYC protein levels in negative control short hairpin RNA (NC-shRNA) and GTPBP4-shRNA cells. C: qRT-PCR assessment of MYC mRNA abundance in control and GTPBP4-knockdown cells. D: Immunoblot showing MYC protein expression in NC-shRNA, GTPBP4-shRNA, and GTPBP4-shRNA cells engineered for ectopic MYC expression (GTPBP4-shRNA+MYC). E: Cycloheximide (CHX) chase assay monitoring MYC protein stability over a 1-hour

time course (CHX concentration: 15 μg/mL) in NC-shRNA and GTPBP4-shRNA cells. F: Immunoblot analysis of MYC protein levels following treatment of GTPBP4-shRNA cells with vehicle control (dimethyl sulfoxide, DMSO), the autophagy inhibitor chloroquine (CQ), or the proteasome inhibitor MG132. G: Time-course assessment of MYC protein accumulation in GTPBP4-shRNA cells exposed to MG132 (10 μM) for the indicated intervals. H: Ubiquitination assay performed in 293T cells co-transfected with plasmids encoding GTPBP4 and MYC; total ubiquitinated MYC species were detected by immunoprecipitation (IP) and immunoblotting with an anti-ubiquitin (Ub) antibody. ***P < 0.001.

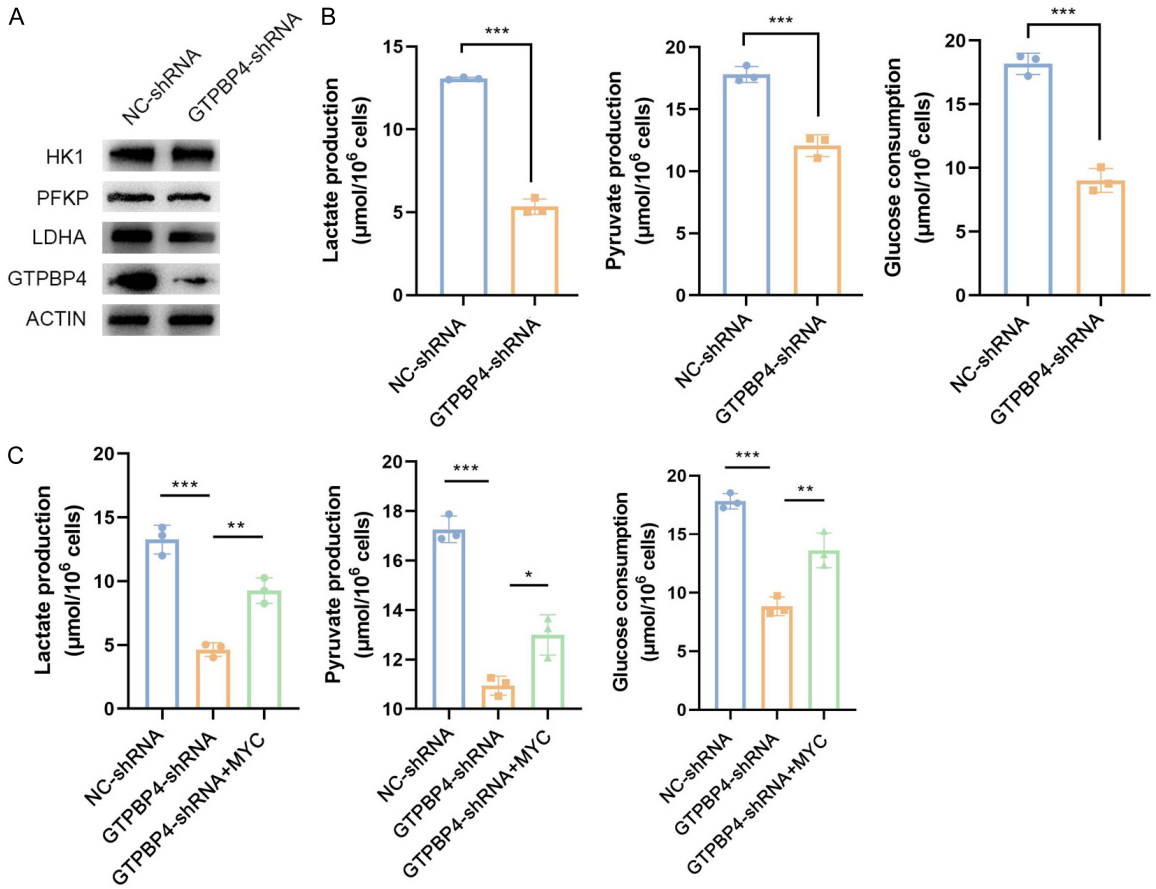

Figure 4. GTPBP4 is associated with MYC-mediated alterations in glycolytic metabolism. A: Immunoblot analysis of key glycolytic enzymes - hexokinase 1 (HK1), phosphofructokinase platelet type (PFKP), and lactate dehydrogenase A (LDHA) - in NC-shRNA and GTPBP4-shRNA cells. B: Quantification of lactate efflux, pyruvate production, and glucose consumption rates in control and GTPBP4-depleted cells. C: Metabolic profiling comparing lactate release, pyruvate generation, and glucose uptake in GTPBP4-shRNA cells versus GTPBP4-shRNA cells with reconstituted MYC expression. *P < 0.05, **P < 0.01, ***P < 0.001.

xenograft model. Male BALB/c athymic nude mice were inoculated with HCT116 cells stably expressing NC-shRNA, GTPBP4-shRNA, or GTPBP4-shRNA plus MYC. Molecular analyses of excised xenografts confirmed that both *GTPBP4* transcript and protein levels were substantially downregulated in the GTPBP4-shRNA group ($P < 0.001$). No significant difference was observed between the GTPBP4-shRNA+MYC group and the NC-shRNA control ($P > 0.05$). MYC messenger RNA (mRNA) and protein expression were significantly reduced in GTPBP4-shRNA tumors but were markedly restored in the GTPBP4-shRNA+MYC rescue cohort ($P < 0.001$) (**Figure 5A**, **5B**). Immunoblotting and immunohistochemical (IHC) staining further demonstrated that expression of the proliferation marker Ki-67, along with glycolytic enzymes LDHA, HK1, and PFKP, was significantly diminished in GTPBP4-shRNA xenografts, whereas these molecular indices were largely recovered in the rescue group ($P < 0.01$) (**Figures 5B**, **6A**).

Metabolic profiling of tumor lysates revealed that lactate and pyruvate production, as well

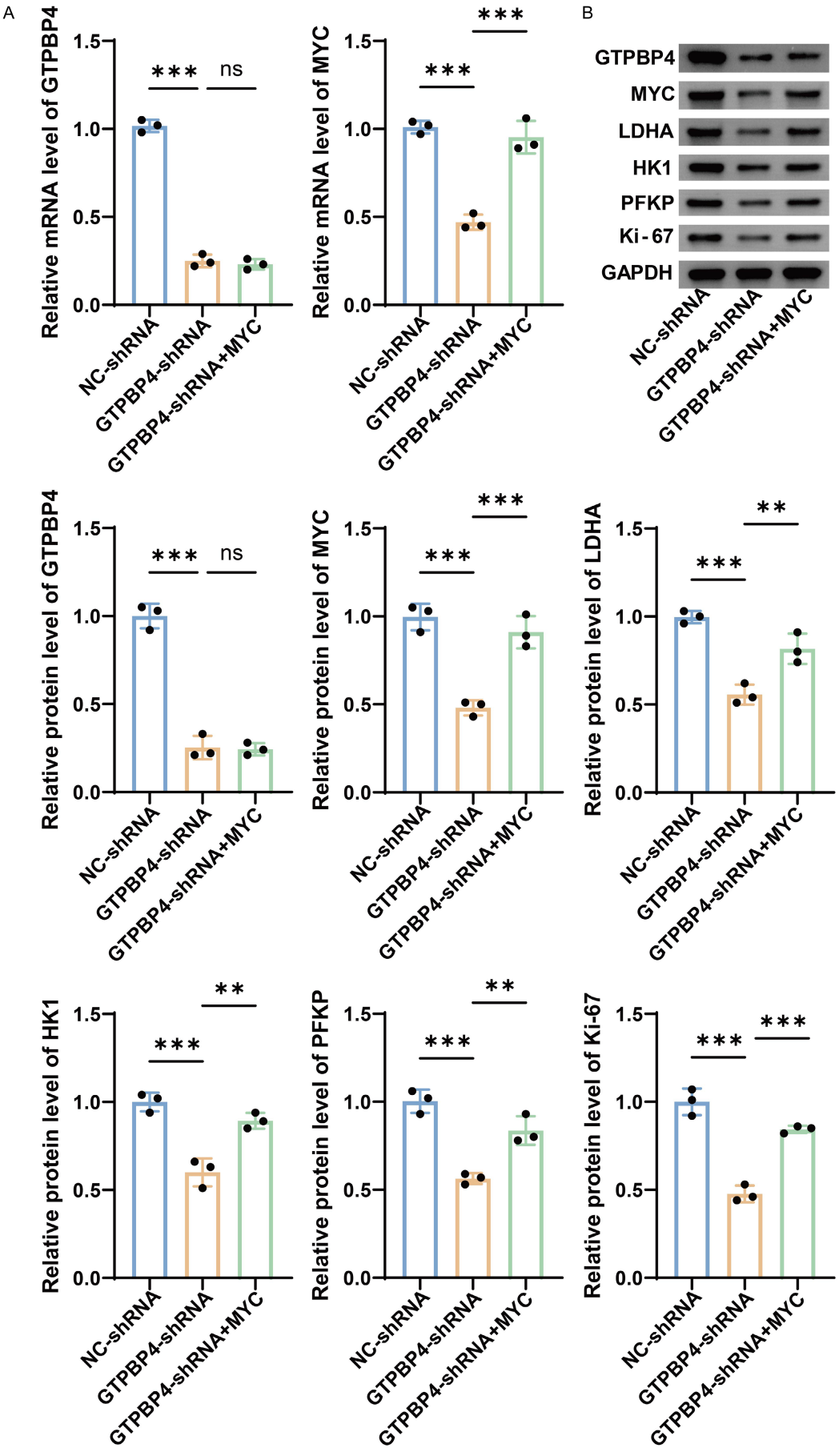
A
B
Relative mRNA level of GTPBP4
Relative mRNA level of MYC
Relative protein level of GTPBP4
Relative protein level of MYC
Relative protein level of LDHA
Relative protein level of HK1
Relative protein level of PFKP
Relative protein level of Ki-67
1.5
1.0
0.5
0.0
***
ns
**
NC-shRNA
GTPBP4-shRNA
GTPBP4-shRNA+MYC
GTPBP4
MYC
LDHA
HK1
PFKP
Ki-67
GAPDH

Figure 5. Expression of GTPBP4, MYC, and downstream molecules in the xenograft tumors. A: qRT-PCR quantification of GTPBP4 and MYC mRNA levels in xenograft tumor lysates derived from athymic nude mice. B: Immunoblot assessment of GTPBP4, MYC, proliferation marker Ki-67, and glycolytic enzymes (LDHA, HK1, PFKP) in xenograft tumor protein extracts. $^{**}P < 0.01$, $^{***}P < 0.001$. ns: not significant.

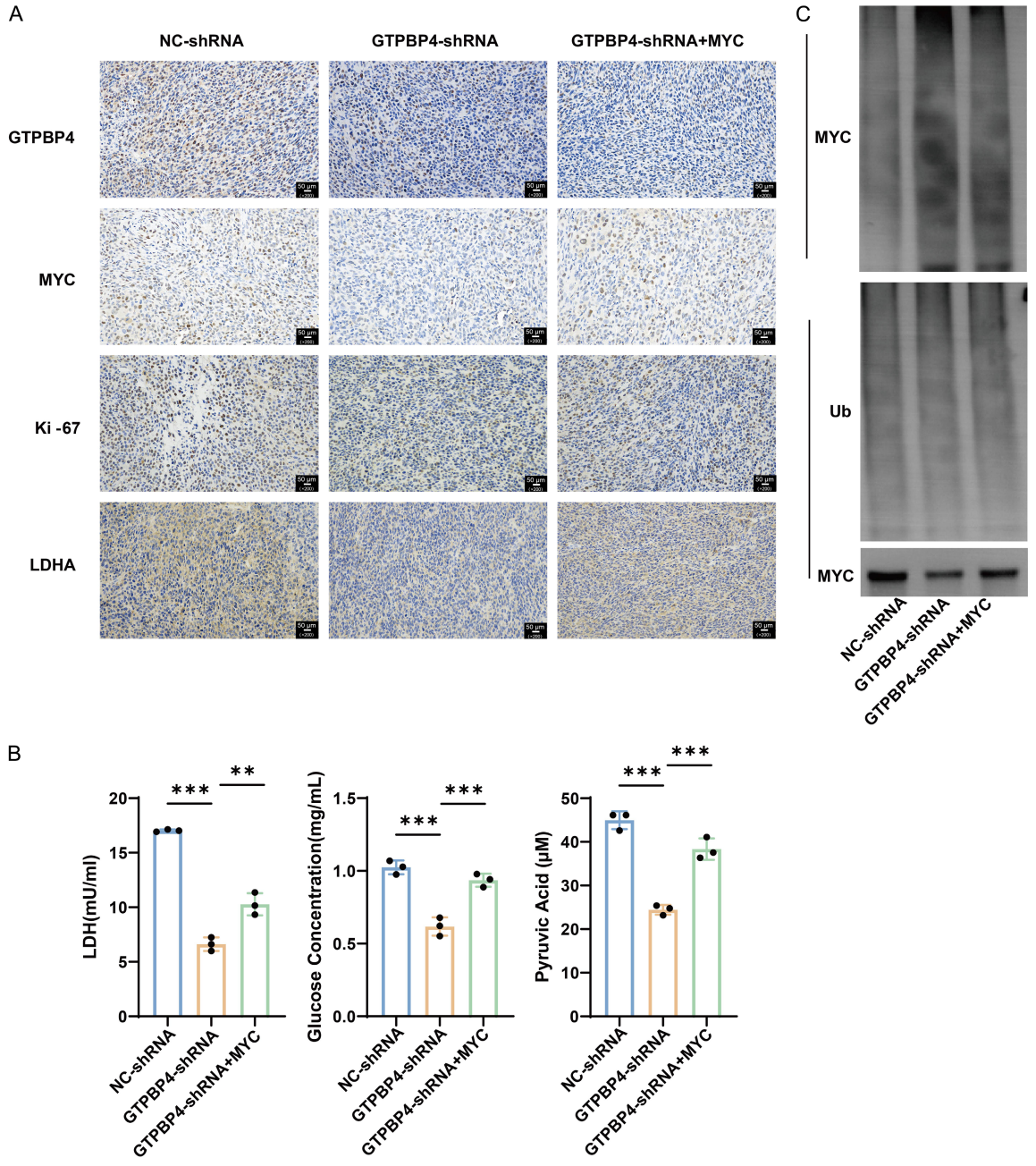

Figure 6. Immunohistochemical detection, metabolic profiling, and MYC ubiquitination status in xenograft tumors. A: Representative IHC micrographs depicting protein localization and relative expression intensity of GTPBP4, MYC, Ki-67, and LDHA within xenograft tumor sections (scale bar = 50 μm, original magnification ×200). B: Ex vivo metabolic assays quantifying glycolytic parameters in freshly excised xenograft tissues. C: Immunoprecipitation analysis assessing the extent of MYC ubiquitination in xenograft tumor lysates derived from the indicated experimental groups. $^{**}P < 0.01$, $^{***}P < 0.001$.

as glucose consumption, were significantly lower in GTPBP4-shRNA xenografts than in controls, with near-complete restoration observed in the GTPBP4-shRNA+MYC group

(**Figure 6B**). Immunoprecipitation (IP) assays confirmed that MYC ubiquitination levels were elevated upon GTPBP4 knockdown, and this increase was attenuated in the rescue setting. Total MYC protein and ubiquitin (Ub) levels remained comparable across groups (**Figure 6C**). Collectively, these in vivo findings corroborate that GTPBP4 positively regulates MYC expression at both transcriptional and post-transcriptional levels, thereby contributing to alterations in glycolytic metabolism and colorectal tumor growth. The ability of MYC overexpression to reverse the phenotypic consequences of GTPBP4 depletion underscores the critical role of the GTPBP4/MYC/glycolysis axis in driving colorectal cancer progression.

Discussion

This study provides a systematic characterization of the expression profile, biological function, and underlying regulatory mechanism of GTP binding protein 4 (GTPBP4) in colorectal cancer. Through coordinated in vitro and in vivo experimentation, we establish a functional link between GTPBP4 and MYC proto-oncogene protein (MYC)-driven alterations in glycolytic metabolism, thereby delineating its contribution to colorectal cancer progression. Initial interrogation of The Cancer Genome Atlas Colon Adenocarcinoma (TCGA-COAD) dataset, corroborated by validation in clinical specimens, revealed pronounced overexpression of GTPBP4 in colorectal tumor tissues, an elevation that correlated significantly with unfavorable patient prognosis. These observations position GTPBP4 as a candidate pro-tumorigenic factor in the pathogenesis of colorectal cancer. In pursuit of the mechanistic basis for this oncogenic activity, correlation analysis uncovered a robust positive association between GTPBP4 and MYC expression.

The MYC transcription factor exerts master regulatory control over aerobic glycolysis and is broadly implicated in the proliferative capacity of cancer cells [18]. The accelerated proliferation characteristic of tumor cells imposes heightened bioenergetic and biosynthetic demands, which are met, at least in part, through reliance on glycolytic metabolism [19]. Prior work has established that diverse genetic elements - including NKD1 [20], OSI-027 [21], RNF8 [22], acetyl-coenzyme A synthetase short-chain family member 2 (ACSS2) [23], and far upstream element-binding protein 1 (FUBP1) [24] - modulate colorectal carcinogenesis via the MYC signaling axis. Moreover, perturbations in MYC ubiquitination dynamics are known to influence disease progression across multiple cancer types. For instance, the long non-coding RNA AFAP1-AS1 has been shown to interact with Smad nuclear interacting protein 1 (SNIP1) to impede c-Myc ubiquitination and degradation, thereby fostering lung cancer cell migration and invasion [25]. Conversely, vitexin promotes c-Myc ubiquitination by disrupting the interaction between inosine monophosphate dehydrogenase 2 (IMPDH2) and c-Myc, consequently restraining colorectal cancer cell motility and invasiveness [26]. In the present study, we demonstrate at the cellular level that GTPBP4 depletion concurrently diminishes MYC transcript abundance, enhances MYC ubiquitination, and accelerates MYC protein turnover. These molecular alterations culminate in the downregulation of glycolytic enzymes and a corresponding attenuation of glycolytic metabolite production. Crucially, ectopic expression of MYC largely abrogated these effects, indicating that GTPBP4 positively regulates MYC expression at both transcriptional and post-transcriptional tiers and is thereby coupled to metabolic reprogramming toward glycolysis.

It is noteworthy that quantitative real-time polymerase chain reaction (qRT-PCR) analyses consistently documented a significant reduction in MYC messenger RNA (mRNA) levels following GTPBP4 knockdown, both in HCT116 and SW620 cell lines and in xenograft tumor lysates. This finding underscores that GTPBP4-mediated regulation of MYC extends beyond the maintenance of protein stability alone. Nonetheless, the current experimental framework does not permit a definitive distinction regarding the precise node of transcriptional or post-transcriptional control - whether GTPBP4 influences MYC transcription initiation, modulates mRNA stability, or impacts other processing events. Likewise, the relative quantitative contributions of transcriptional versus post-translational regulation to the net abundance of MYC protein remain to be resolved. Further investigation employing assays such as nuclear run-on, chromatin immunoprecipitation (ChIP), or mRNA decay rate measurements will

be required to dissect these layered regulatory mechanisms. Despite this mechanistic nuance, the collective data support a model in which GTPBP4 functions upstream of MYC to sustain its expression and, by extension, the glycolytic phenotype associated with aggressive colorectal cancer.

In vivo functional validation was performed using a subcutaneous xenograft model in athymic nude mice. GTPBP4 depletion led to a marked reduction in both tumor volume and mass. Concordantly, xenograft tissues from the GTPBP4-short hairpin RNA (shRNA) group exhibited significantly decreased expression of MYC, the proliferation marker Ki-67, and glycolytic enzymes - lactate dehydrogenase A (LDHA), hexokinase 1 (HK1), and phosphofructokinase platelet type (PFKP). Glycolytic indices, including lactate production and glucose consumption, were correspondingly attenuated. In contrast, co-expression of MYC in the GTPBP4-knockdown background effectively rescued these suppressive effects, restoring tumor growth, cellular proliferation, and glycolytic activity to levels approximating those of the control cohort. Immunoprecipitation (IP) assays conducted on xenograft lysates further corroborated that GTPBP4 depletion substantially elevates MYC ubiquitination levels, an effect that is blunted by concomitant MYC overexpression. Total ubiquitin (Ub) abundance remained invariant across experimental groups. These in vivo observations recapitulate the cellular findings and reinforce a model wherein GTPBP4 knockdown enhances MYC ubiquitination, diminishes MYC protein abundance, and curtails glycolytic metabolism. The convergence of in vitro and in vivo evidence supports a functional paradigm in which GTPBP4 positively regulates MYC expression, thereby contributing to altered glycolytic metabolism and driving colorectal cancer cell proliferation and subcutaneous tumor growth. It is important to acknowledge, however, that the subcutaneous xenograft model employed herein permits conclusions pertaining only to tumor growth and cannot recapitulate the more complex facets of colorectal cancer biology, including metastatic dissemination, local invasion, or dynamic interactions within the tumor microenvironment. Thus, while the present findings delineate a GTPBP4/MYC/glycolysis axis of clear relevance, a complete portrait of the oncogenic mechanism awaits further elucidation.

This study establishes that GTPBP4 depletion influences both MYC ubiquitination status and MYC transcript abundance, yet the precise molecular underpinnings of this dual regulation remain to be defined. The available data do not permit a quantitative dissection of the relative contributions of transcriptional, post-transcriptional, and post-translational control to GTPBP4-mediated MYC regulation. As GTPBP4 is not known to possess intrinsic E3 ubiquitin ligase or deubiquitinase activity, it likely exerts its effects indirectly through physical interactions with other proteins - candidate E3 ligases, deubiquitinating enzymes, or transcriptional regulators - that govern MYC expression and stability. Future investigations employing co-immunoprecipitation coupled with mass spectrometry (Co-IP/MS) will be valuable for identifying the GTPBP4 interactome and pinpointing the direct molecular mediators of MYC regulation [27]. Furthermore, the prognostic relevance and elevated expression of GTPBP4 demonstrated here rely on TCGA dataset and a limited set of clinical tissue specimens, and in vivo validation was restricted to a subcutaneous xenograft approach. Future studies should expand clinical cohort sizes and integrate orthogonal approaches - including IHC on tissue microarrays and metabolomic profiling - to interrogate correlations between GTPBP4 abundance, MYC levels, glycolytic metrics, and clinicopathological parameters such as tumor stage and histological grade. Complementary analyses in orthotopic xenograft models and genetically engineered mouse models will be essential to more faithfully assess the role of GTPBP4 in the natural history of colorectal cancer and to furnish more robust evidence supporting its translational potential.

Conclusion

This study provides in vitro and in vivo evidence that GTP binding protein 4 (GTPBP4) is overexpressed in colorectal cancer and that high expression correlates with poor clinical outcome. Mechanistically, GTPBP4 positively regulates MYC proto-oncogene protein (MYC) expression at both the transcriptional and post-transcriptional levels - at least in part by

restraining MYC ubiquitination and preserving its protein stability - and is thereby functionally coupled to alterations in glycolytic metabolism that promote colorectal cancer progression. Ectopic expression of MYC reverses the phenotypic consequences of GTPBP4 depletion. These findings not only expand the mechanistic landscape of metabolic reprogramming in colorectal cancer but also nominate GTPBP4 as a potential therapeutic target. The work provides an experimental foundation for future efforts aimed at developing therapeutic strategies directed against GTPBP4 or its downstream regulatory circuitry.

Disclosure of conflict of interest

None.

Address correspondence to: Jianzhong Deng, Department of Oncology, Wujin Hospital Affiliated to Jiangsu University, Changzhou 213017, Jiangsu, China. Tel: +86-0519-85579150; E-mail: dengjianzhong@wjrmyy.cn

References

[1] Meyer U, Rönnpagel V, Grammbauer S, von Lucadou M, Rauch-Kröhnert U, Schwedhelm E, Dombrowski F, Ritter C and Rauch BH. Significance of FXa and its receptor PAR2 for the growth of colon cancer cells in vitro and in vivo. Front Oncol 2025; 15: 1631350.

[2] Du Y, Kuang Y, Meng X, Zheng B, Chen Q, Yan Q and Li J. CYP2S1 knockout promotes intestinal tumor growth in APCMin/+ mice and its clinical significance. J Cancer 2025; 16: 3128-3140.

[3] Zeng C, Qi G, Shen Y, Li W, Zhu Q, Yang C, Deng J, Lu W, Liu Q and Jin J. DPEP1 promotes drug resistance in colon cancer cells by forming a positive feedback loop with ASCL2. Cancer Med 2023; 12: 412-424.

[4] Zhou Q, Yin Y, Yu M, Gao D, Sun J, Yang Z, Weng J, Chen W, Atyah M, Shen Y, Ye Q, Li CW, Hung MC, Dong Q, Zhou C and Ren N. GTPBP4 promotes hepatocellular carcinoma progression and metastasis via the PKM2 dependent glucose metabolism. Redox Biol 2022; 56: 102458.

[5] Zhang N, Shen H, Huang S, Wang F, Liu H, Xie F, Jiang L and Chen X. LncRNA FGD5-AS1 functions as an oncogene to upregulate GTPBP4 expression by sponging miR-873-5p in hepatocellular carcinoma. Eur J Histochem 2021; 65: 3300.

[6] Liu WB, Jia WD, Ma JL, Xu GL, Zhou HC, Peng Y and Wang W. Knockdown of GTPBP4 inhibits cell growth and survival in human hepatocellular carcinoma and its prognostic significance. Oncotarget 2017; 8: 93984-93997.

[7] Li L, Pang X, Zhu Z, Lu L, Yang J, Cao J and Fei S. GTPBP4 promotes gastric cancer progression via regulating P53 activity. Cell Physiol Biochem 2018; 45: 667-676.

[8] Hu Y, Xie J, Chen L, Tang Q, Wei W, Lin W, Du W, Xiang T, Yin L and Ji J. Integrated analysis of genomic and transcriptomic profiles identified the role of GTP binding protein-4 (GTPBP4) in breast cancer. Front Pharmacol 2022; 13: 880445.

[9] Wu J, Chen G, Wang W, Yang Y, Yuan Y, Shang A, Quan W and Wang L. GTPBP4: a new therapeutic target gene promotes tumor progression in non-small cell lung cancer via EMT. J Oncol 2022; 2022: 2164897.

[10] Li C, Liu FY, Shen Y, Tian Y and Han FJ. Research progress on the mechanism of glycolysis in ovarian cancer. Front Immunol 2023; 14: 1284853.

[11] Niu Z, He J, Wang S, Xue B, Zhang H, Hou R, Xu Z, Sun J, He F and Pei X. Targeting glycolysis for treatment of breast cancer resistance: current progress and future prospects. Int J Biol Sci 2025; 21: 2589-2605.

[12] Kooshan Z, Cárdenas-Piedra L, Clements J and Batra J. Glycolysis, the sweet appetite of the tumor microenvironment. Cancer Lett 2024; 600: 217156.

[13] Li M, Yu J, Ju L, Wang Y, Jin W, Zhang R, Xiang W, Ji M, Du W, Wang G, Qian K, Zhang Y, Xiao Y and Wang X. USP43 stabilizes c-Myc to promote glycolysis and metastasis in bladder cancer. Cell Death Dis 2024; 15: 44.

[14] Liu F, Chen J, Li K, Li H, Zhu Y, Zhai Y, Lu B, Fan Y, Liu Z, Chen X, Jia X, Dong Z and Liu K. Ubiquitination and deubiquitination in cancer: from mechanisms to novel therapeutic approaches. Mol Cancer 2024; 23: 148.

[15] Awan AB, Osman MJA and Khan OM. Ubiquitination enzymes in cancer, cancer immune evasion, and potential therapeutic opportunities. Cells 2025; 14: 69.

[16] De Silva ARI and Page RC. Ubiquitination detection techniques. Exp Biol Med (Maywood) 2023; 248: 1333-1346.

[17] Mansour MA. Ubiquitination: friend and foe in cancer. Int J Biochem Cell Biol 2018; 101: 80-93.

[18] Hsieh AL, Walton ZE, Altman BJ, Stine ZE and Dang CV. MYC and metabolism on the path to cancer. Semin Cell Dev Biol 2015; 43: 11-21.

[19] Han X, Ren C, Lu C, Qiao P, Yang T and Yu Z. Deubiquitination of MYC by OTUB1 contributes to HK2 mediated glycolysis and breast tumorigenesis. Cell Death Differ 2022; 29: 1864-1873.

[20] Lu W, Tang J, Wang Y, Gu X, Zhang H, Liu Y, Xiao Y, Zhu Q, Deng J, Shen Y, Jiang A, Xu Y, Jin J, Hou Y and Liu Q. NKD1 enhances colon cancer progression by inhibiting the autophagic degradation of MYC. Cell Death Dis 2025; 16: 532.
[21] Lou J, Lv JX, Zhang YP and Liu ZJ. OSI-027 inhibits the tumorigenesis of colon cancer through mediation of c-Myc/FOXO3a/PUMA axis. Cell Biol Int 2022; 46: 1204-1214.
[22] Ren L, Zhou T, Wang Y, Wu Y, Xu H, Liu J, Dong X, Yi F, Guo Q, Wang Z, Li X, Bai N, Guo W, Guo M, Jiang B, Wu X, Feng Y, Song X, Zhang S, Zhao Y, Cao L, Han S and Xing C. RNF8 induces beta-catenin-mediated c-Myc expression and promotes colon cancer proliferation. Int J Biol Sci 2020; 16: 2051-2062.
[23] Park YR, Jee W, Park SM, Kim SW, Jung JH, Kim H, Kim KI and Jang HJ. Acetylcorynoline induces apoptosis and G2/M phase arrest through the c-Myc signaling pathway in colon cancer cells. Int J Mol Sci 2023; 24: 17589.
[24] Wang S, Wang Y, Li S, Nian S, Xu W and Liang F. Far upstream element -binding protein 1 (FUBP1) participates in the malignant process and glycolysis of colon cancer cells by combining with c-Myc. Bioengineered 2022; 13: 12115-12126.
[25] Zhong Y, Yang L, Xiong F, He Y, Tang Y, Shi L, Fan S, Li Z, Zhang S, Gong Z, Guo C, Liao Q, Zhou Y, Zhou M, Xiang B, Li X, Li Y, Zeng Z, Li G and Xiong W. Long non-coding RNA AFAP1-AS1 accelerates lung cancer cells migration and invasion by interacting with SNIP1 to upregulate c-Myc. Signal Transduct Target Ther 2021; 6: 240.
[26] Ding XJ, Cai XM, Wang QQ, Liu N, Zhong WL, Xi XN and Lu YX. Vitexicarpin suppresses malignant progression of colorectal cancer through affecting c-Myc ubiquitination by targeting IMPDH2. Phytomedicine 2024; 132: 155833.
[27] Ritorto MS, Ewan R, Perez-Oliva AB, Knebel A, Buhrlage SJ, Wightman M, Kelly SM, Wood NT, Virdee S, Gray NS, Morrice NA, Alessi DR and Trost M. Screening of DUB activity and specificity by MALDI-TOF mass spectrometry. Nat Commun 2014; 5: 4763.